Fuel Processing Technology 167 (2017) 663–669

Contents lists available at ScienceDirect

Fuel Processing Technology

journal homepage: www.elsevier.com/locate/fuproc

Impact of HTC reaction conditions on the hydrochar properties and CO_2 gasification properties of spent grains

Markus Ulbrich[a,*], Dieter Preßl[a], Sebastian Fendt[a], Matthias Gaderer[c], Hartmut Spliethoff[a,b]

[a] Technical University of Munich, Institute for Energy Systems, Boltzmannstraße 15, Garching 85748, Germany
[b] ZAE Bayern, Walter-Meißner-Straße 15, Garching 85748, Germany
[c] Technical University of Munich, Institute for Regenerative Energy Systems, Schulgasse 16, Straubing 94315, Germany

ARTICLE INFO

Keywords:
Biomass pretreatment
Renewable energies
Hydrothermal carbonization
Gasification kinetics
CO_2 gasification

ABSTRACT

The impact of residence time and temperature during hydrothermal carbonization (HTC) on hydrochar properties and CO_2 gasification properties has been studied for brewers' spent grain (BSG), treated at temperatures from 180 °C to 280 °C and residence times from 0.5 to 12 hours. Lower heating values (LHV) of the hydrochars are found to increase to values of bituminous coal and anthracite as reaction severity increases. Temperature is found to have a greater influence on the LHV of the hydrochar than residence time. Mass and energy yields decrease with increasing reaction severity. With higher reaction severity decreased molar O/C and H/C ratios as well as decreased volatile contents and increased fixed carbon contents are observed. The influence of residence time is more pronounced for the formation of fixed carbon, main carbonization reactions occur for a reaction severity greater than 180 °C and 0.5 hours. Char reactivity is found to decrease with increasing carbonization reaction severity with a strong influence of both residence time and temperature due to the formation of fixed carbon in the hydrochar. Activation energies are decreased with increased carbonization temperature but only mildly affected by residence time. Hereby the catalytic influence of ash compounds has to be further determined.

1. Introduction

As part of the ongoing transition to renewable energy, the German government set its goals to provide 35% of the gross electricity consumption from renewable energy sources by 2020 [1]. In 2014, 27.4% of the energy was produced from renewable sources, of which 8.5% originated from biomass [1,2]. However, due to the large diversity of biomass and unfavorable fuel properties, a significant amount of the available bioenergy potential, especially the potential of biomasses with high moisture contents, remains unused. The biggest hurdles regarding thermal usage have proven to be high moisture contents, high corrosion potential because of high chlorine and alkali contents and extensive fouling and slagging due to low ash fusion temperatures [3]. Moreover, degradation during storage and low energy density strongly limit the economic feasibility of using these biomasses for thermochemical conversion processes. In this context, biomass upgrading technologies such as hydrothermal carbonization (HTC) or torrefaction (TF) have gained renewed interest in recent years.

Hydrothermal carbonization was discovered by Friedrich Bergius in 1913 as a method to recreate natural coalification in a hydrothermal environment under typical process conditions of 180 °C–250 °C and residence times from 1 h to 12 h [4–7]. Under these conditions, the liquid high pressure water changes its chemical properties and a complex reaction network of decomposition and polymerization of the hemicellulose and cellulose, and degradation of the lignin transform the biomass into a solid product, often referred to as hydrochar, which is found to exhibit improved fuel properties [6,8,9]. Hydrochars generally show higher heating values, higher ash fusion temperatures and in some cases reduced sulfur and nitrogen contents compared to the raw biomass [8,10]. Also the hydrophobicity of the hydrochars is increased, facilitating the drying process and strongly increasing the storage stability [11]. Compared to TF, the efficiency of HTC, due to the necessary immersion in water, favors the use of wet biomass and therefore presents a possibility of a profitable usage of wet biomass residues in energetic processes.

A promising biomass in this context is brewers' spent grains (BSG) with an annual production of 2 Mt in Germany in 2010 [12]. Currently BSG is mainly used as feed for cattle but a decreasing number of livestock and the possibility of energy generation for the brewing process open an attractive pathway for energetic use of this biomass [13]. The HTC process itself and its impact on the solid product have been examined by various studies for many different types of biomass and a

* Corresponding author at: Lehrstuhl für Energiesysteme, Technische Universität München, Boltzmannstrasse 15, Garching 85748, Germany
E-mail address: Markus.Ulbrich@tum.de (M. Ulbrich).

http://dx.doi.org/10.1016/j.fuproc.2017.08.010
Received 20 October 2016; Received in revised form 18 July 2017; Accepted 3 August 2017
Available online 16 August 2017
0378-3820/

wide range of parameters [7,14-17]. The use of BSG in HTC processes was first examined by Heilmann et al. as an alternative route to drying and combustion, yielding hydrochars with high energy contents at relatively mild conditions [18]. Further investigations in HTC of BSG were performed by Poerschmann et al. and Baskyr et al., giving a detailed picture on the chemistry of the process and proposing a way to treat the process water [19,20]. The first part of this study extends the findings of the previous studies to wider range of process parameters and gives a detailed picture of the impact of reaction conditions on fuel properties, which are important for thermochemical conversion processes.

A new approach to thermochemical conversion of biomass is entrained flow gasification, which has the advantage of high and fast conversion, a high efficiency and low tar generation [21]. The resulting product gas then can be subject to either cogeneration (CHP), conversion to synthetic natural gas or provision of syngas. For this type of gasification an easily grindable, high grade fuel is required, all of which are features reported from hydrochars. Tremel et al. reported a potential conversion of hydrochars made from beech wood in an entrained flow gasifier with conversions of 84%–88 % at temperatures from 1000 °C to 1400 °C [21]. Gunarathne et al. reported a general feasible conversion in a lab-scale gasification setup [22]. However, a link between HTC reaction conditions and the gasification behavior of the resulting hydrochars is still missing. For this reason the second part of this study focuses on the effect of process conditions on the CO_2 gasification reactivity of chars, obtained from pyrolysis of the hydrochars.

2. Experimental method

HTC experiments are carried out in a stirred mini batch reactor with a volume of 600 mL designed for a temperature range of up to 350 °C and a pressure range of up to 200 bar. Temperature is controlled with three heating sleeves with a power of 700 W each. The system is pressurized with argon (4.6 purity) and the pressure is kept constant throughout the process with a backpressure regulator. The biomass used for the experiments is BSG provided by a local brewery. Proximate and ultimate analysis for the biomass is shown in Table 1.

For the HTC experiments, the biomass is immersed in deionized water with a concentration of 10 g dry substance per 100 mL and poured into the reactor. The system is then pressurized, brought to reaction temperature at a heating rate of 7 K min^{-1} and held at the specified residence time. The reactor is cooled down after the reaction and the slurry is filtered and dried to isolate the solid product. Proximate analysis is done according to industrial standard methods DIN 51718, DIN 51719 and DIN 51720, ultimate analysis is done according to industrial standard methods DIN 51900-1 and DIN 51732.

Table 1
Fuel properties of brewers' spent grains.

Proximate analysis (wt.%)	
Ash content (dry)	3.8
Volatile matter content (dry)	83.9
Moisture content (as received)	80.0
Fixed Carbon (dry)	12.3
Ultimate analysis (wt.%, dry)	
C	50.4
H	6.4
N	4.1
S	0.7
O	34.6
Cl[1]	0.03
Caloric Properties (MJ kg^{-1}, dry)	
LHV	21.5
HHV	23.3

[1] Not included in CHNSO balance

Gasification properties are analyzed in an atmospheric thermogravimetric analyzer (TGA). To ensure uniform pyrolysis and high heating rates, sample pyrolysis is done at 1100 °C for 7 min in a preheated muffle furnace under inert atmosphere. The pyrolysis method is based on DIN 51719 with the high temperature chosen to avoid pyrolysis during gasification experiments. 20 mg of the resulting char sample is then distributed evenly on the sample holder of the TGA with no particles lying on top of each other to minimize mass transport limitation effects. Subsequently, the TGA is heated to the specified temperature with a heating rate of 20 K min^{-1} under nitrogen atmosphere and a volume flow of 200 cm^3 min^{-1} and held constant for at least 30 min to avoid ongoing pyrolysis during gasification. When the mass signal remained constant during holding period, the nitrogen flow is switched to 200 cm^3 min^{-1} CO_2 and the mass signal is recorded. If pyrolysis from the char is detected during the holding period, the sample is discarded. When necessary the mass signal is smoothed using the Gaussian method as proposed by *Chen et al.* [23].

The temperature range for the measurement of the reactivity and the activation energy is determined by heating the samples from room temperature to 1100 °C with a heating rate of 20 K min^{-1} with 200 cm^3 min^{-1} CO_2 volume flow until the sample weight remains constant. After adjustment of the weight loss curve with the temperature related buoyancy effects the start of the CO_2 reaction can be determined. Based on this temperature the starting temperature for the activation energy measurement is selected. The reactivity of the char samples is measured isothermally at 20% char conversion. Linear regression of the mass loss curve from 15% to 20% conversion proves to be the best method to determine the mass loss rate, since the mass loss rate is constant in this range. The mass loss signal received from the thermogravimetric analyzer (TGA) is averaged from 15% conversion to 25% conversion to get the reaction rate at 20% conversion. In this conversion range the mass signal decreases linearly ($R^2 > 0.999$, error of the slope < 0.01 %), so that the conversion rate at 20 % can be obtained with a high precision of appr. 0.5% for two char samples with the same HTC-reaction conditions. After the starting temperature of the CO_2 reaction is found to be appr. 850 °C for all samples, the reactivity is measured at 850 °C, 950 °C and 1050 °C. The observed reaction rate r_{obs} is determined with the derivative of the weight loss curve as shown in Eq. (1) with m as the recorded mass of the sample in mg and X the char conversion.

$$r_{obs} = \frac{1}{m}\cdot\frac{dm}{dt} = \frac{1}{1-X}\cdot\frac{dX}{dt} \tag{1}$$

The activation energies E_A of the CO_2 reaction were modeled based on the Arrhenius equation as suggested by *Irfan et. al.* [24]. In this simplified modeling approach the reaction order is assumed to be 1 and the activation energy $E_{A,obs}$ in kJ kg^{-1} is modeled as an observed activation energy from linear regression of $\ln(r_{obs})$ measured at 850 °C, 950 °C and 1050 °C, the universal gas constant R and temperature T in K according to Eq. (2).

$$E_{A,obs} = -R\cdot\frac{\sum_{i=1}^{N}\left\{\left(\frac{1}{T_i}-\frac{1}{\overline{T}}\right)\cdot\left(\ln r_{obs,i}-\overline{\ln r_{obs}}\right)\right\}}{\sum_{i=1}^{N}\left\{\frac{1}{T_i}-\frac{1}{\overline{T}}\right\}^2} \tag{2}$$

The determination of the activation energy proved to be reproducible with a deviation of 1.5% for two different samples with the same HTC-reaction conditions. However, the reproducibility test could not be done for all samples due to the long experimental procedure of hydrothermal carbonization followed by pyrolysis and gasification experiments so an error of 1.5% is assumed for all activation energies. The reactivity of the most reactive char samples is additionally determined at 650 °C and the Arrhenius plot of the respective samples is checked for linearity to ensure the absence of mass transport limitations.

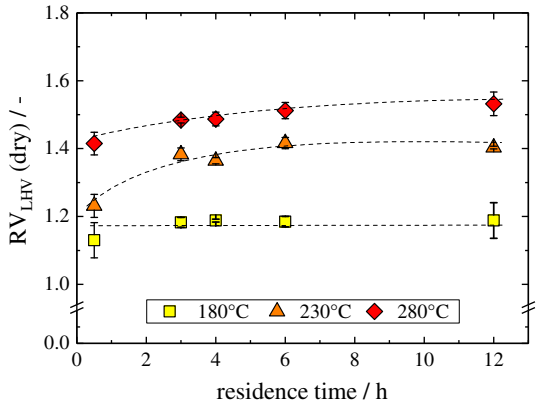

Fig. 1. Relative LHV (dry) of BSG hydrochars for reaction temperatures 180 °C, 230 °C and 280 °C versus residence time.

3. Results and discussion

3.1. Hydrochar properties

The spent grains are treated at temperatures of 180 °C, 230 °C and 280 °C and residence times of 0.5, 3, 4, 6 and 12 h. The carbonized biomass is referred to as hydrochar. For better comparison, the fuel property data are presented in relative values according to Eq. (3). The absolute values in each figure can be obtained using Table 1.

$$RV_i = \frac{X_{hydrochar,dry}}{X_{sample,dry}} \tag{3}$$

With RV_i the relative fuel property and $X_{hydrochar,dry}$, $X_{sample,dry}$ the fuel property of the hydrochar and raw sample, respectively.

Fig. 1 shows the relative lower heating values (RV_{LHV}) (see Eq. (3)) of the resulting hydrochar samples.

All samples show significantly increased heating values with increased reaction severity ranging from a 1.13-fold increase at 180 °C and 0.5 h to 1.58 at 280 °C and 12 h. For all temperatures, residence time proves to have a fairly low influence on the heating value remaining nearly constant from 3 to 12 h at RV_{LHV}s of 1.18, 1.40 and 1.53 for the reaction temperatures 180 °C, 230 °C and 280 °C, respectively. Higher temperature effects the RV_{LHV} positively at all residence times with a more pronounced increase from 180 °C to 230 °C of 1.19 to 1.42 than from 230 °C to 280 °C of 1.41 to 1.52 representative for 6 h residence time. The heating values of the hydrochars are found to be in the range of lignite (22–26 MJ kg^{-1} [25]) for low reaction severity and anthracite (> 30MJ kg^{-1} [25]) for high reaction severity. Literature data by Baskyr et al. and Poerschmann et al. calculated from empirical correlations seems to show similar trends for BSG with a RV_{LHV} of 1.31–1.34 at reaction conditions of 200 °C and a RV_{LHV} of 1.42–1.47 at reaction conditions of 240 °C [19,20]. The recovered solids (mass yield, MY) and the recovered chemical energy (energy yield, EY) after the process is examined according to Eqs. (4) and (5) with $m_{hydrochar,dry}$ and $m_{sample,dry}$ the dry masses of the hydrochar and the sample in g and $LHV_{hydrochar,dry}$ and $LHV_{sample,dry}$ the lower heating values of the hydrochar and the sample in MJ kg^{-1}.

$$MY_{dry} = \frac{m_{hydrochar,dry}}{m_{sample,dry}} \tag{4}$$

$$EY_{dry} = MY \cdot \frac{LHV_{hydrochar,dry}}{LHV_{sample,dry}} \tag{5}$$

Fig. 2 shows the resulting mass and energy yields.

The obtained solid mass yield shows a significant sensitivity to temperature but is only mildly affected by increasing residence time. The mass yield remains approximately constant over residence time at the lowest reaction temperature of 180 °C at appr. 0.52. By increasing

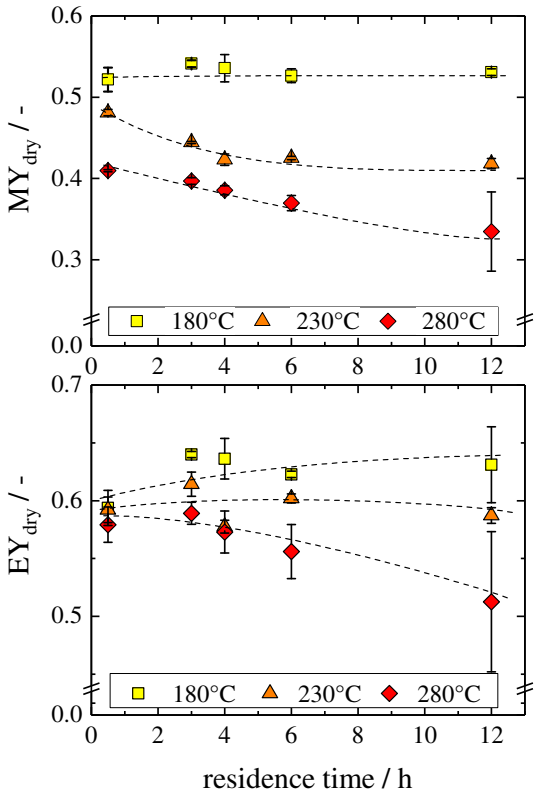

Fig. 2. Mass yield and energy yield of BSG hydrochars for reaction temperatures 180 °C, 230 °C and 280 °C versus residence time.

the temperature from 180 °C to 230 °C the mass yield significantly decreases from 0.52 to a mean value of 0.42 for residence times 2–12 h. With the temperature increased from 230 °C to 280 °C the decrease in mass yield is less pronounced decreasing from 0.41 at 0.5 h to 0.34 at 12 h. This trend is not reflected at 0.5 h residence time due to the heating time of the reactor where the reaction progress especially for the high temperature samples is already significantly more advanced than for the lower temperature sample. At 280 °C and 12 h residence time the reproducibility of the mass yield is affected negatively by the beginning liquefaction of BSG, often resulting in total dissolution of the biomass. However, the fuel properties of the hydrochars show good reproducibility.

The energy yield is found to be fairly constant in the range of appr. 0.6 for reaction temperatures 180 °C and 230 °C for all residence times and for residence times shorter than 6 h at 280 °C. Occurring trends for the energy yield at 180 °C and 230 °C are within the uncertainty of this parameter caused by the combined analysis errors from LHV and the solid mass yield. With the beginning liquefaction of the sample for residence times greater than 6 h at 280 °C, a substantial fraction of organic matter compounds of the biomass are dissolved in the water phase. This results in a decreased energy yield of the hydrochar with a mean value of 0.51 ± 0.06 at 12 h. The relatively high uncertainty for this parameter set is caused by the observed liquefaction of the sample and the therefore poor reproducibility of the mass yield.

The carbonization leads to a change in the elemental composition of the biomass displayed in Fig. 3 where the molar ratios of O/C and H/C are shown according to the method by *D.W. van Krevelen* to examine the degree of coalification and the reaction pathways of decarboxylation, dehydration and demethanation during the carbonization [26].

Compared to raw biomass with a molar O/C ratio of 0.52 and a molar H/C ratio of 1.50 oxygen is removed from the biomass decreasing the O/C ratio to 0.33 at 180 °C and 0.5 h and to a minimum of 0.08 for 280 °C and 12 h, thus increasing the heating values of the hydrochars. According to Fig. 3 the predominant reaction mechanism for 180 °C and

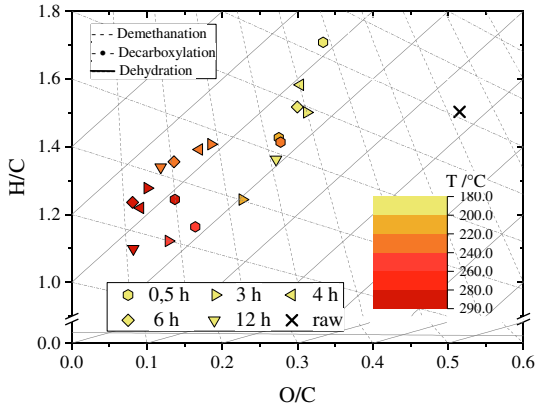

Fig. 3. Van Krevelen diagram of BSG hydrochars for reaction temperatures 180 °C, 230 °C and 280 °C and residence times from 0.5 h to 12 h.

0.5 h is decarboxylation. At temperatures of 150 °C it is assumed that carbon dioxide is released from the biomass matrix via elimination of unstable carboxyl groups [27]. Significant reactions occur at temperatures above 180 °C where hemicellulose (180 °C), cellulose (220 °C) and lignin (180 °C–220 °C) are hydrolyzed. During the reaction, structures resembling the chemical structure of coal are formed by polyreactions, aromatization of hydrolyzed intermediates and dehydration of the biomass matrix [8,27]. Reaction severity greater than 180 °C and 0.5 h predominantly leads to dehydration reactions resulting in a minimal O/C of 0.08 and a minimal H/C of 1.10 which is in the region of low rank bituminous coal for O/C (0.115 [26]) and peat for the H/C ratio (1.1 [26]). In comparison to Fig. 1, residence time shows a more significant influence on the carbonization degree than on the heating values. At 180 °C a decrease of mostly the H/C ratio can be seen until a residence time of 12 h suggesting internal structural transformation in the solid body of the samples rather than extensive removal of oxygen. This effect is less apparent for higher temperatures.

A more detailed picture of the influence of the HTC reaction conditions on the chemical composition of the hydrochars can be derived from the elemental analysis as shown in Fig. 4. For a better comparability carbon, hydrogen and oxygen are given as a relative elemental analysis (REA) according to Eq. (3).

The previously seen progressing coalification with increasing reaction severity is reflected in the increased carbon content and decreased oxygen content. Here, the carbon content almost exactly shows the trends and values seen for the RV_{LHV} (see Fig. 1) since, with carbon as the main energy source in hydrochars during thermal conversion, these values are directly related. Symmetrically, oxygen is removed from the hydrochar with increasing reaction severity. At 180 °C relative oxygen content was found to decrease to a fraction of 0.75 at 0.5 h further decreasing with increasing residence time to 0.66 at 12 h. For higher temperatures the influence of residence time becomes more apparent with the reduction of the relative oxygen content from 0.67 to 0.33 at 230 °C and from 0.37 to 0.23 at 280 °C. Taking into account the observed mass yields and the suggested main pathway of dehydration (see Fig. 3) the absolute carbon content is decreased to a lesser degree than the absolute oxygen content thus resulting in a decreased O/C ratio and an increased heating value of the solid product. The relative hydrogen content in the hydrochars is increased to values between 1.19 and 1.32 for all temperatures and residence times and only exhibits weak trends. Since the relative hydrogen content is calculated based on mass fractions the uncertainty of this value is significantly higher than for oxygen and carbon. However, due to the decreased mass yield with increasing reaction severity the absolute amount of hydrogen is also decreased to a lesser degree than the absolute carbon resulting, in accordance with Fig. 3, in a decreased H/C ratio and therefore a more uniform carbon structure and an increased coal rank. The structural transition due to

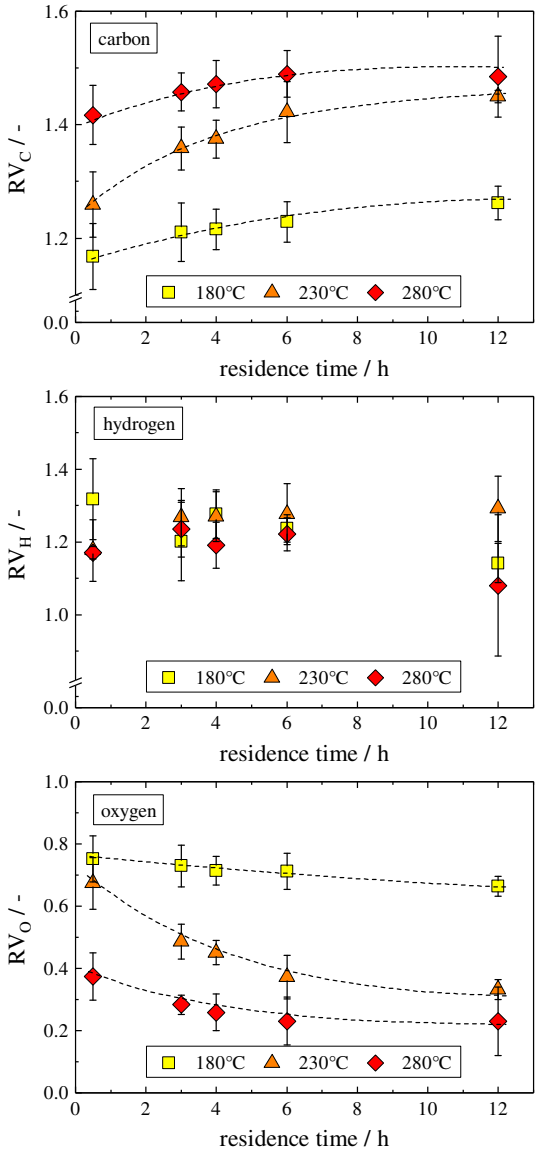

Fig. 4. Relative carbon, hydrogen and oxygen content of BSG hydrochars for reaction temperatures 180 °C, 230 °C and 280 °C versus residence time.

the HTC can also be seen in Fig. 5a) and b) where the relative volatile content and the relative fixed carbon content of the resulting coal samples are displayed.

With higher reaction severity the progressing coalification of the fuel structure results in a reduced content of volatile components and an increased content of fixed carbon. At low reaction severity, the volatile and fixed carbon content nearly resembles the raw biomass. This suggests, in accordance with Fig. 3 at 180 °C and 0.5 h that the main structural coalification reactions occur at higher temperatures and longer residence times. For higher reaction severity the relative volatile content is decreased from 0.97 at 180 °C and 0.5 h to a minimum of 0.70 at 280 °C and 4 h. The minimum is expected to be at 280 °C and 12 h but due to the weak influence of residence time at 280 °C the minimum at 4 h is likely to be a statistical deviation. For the volatile content the same trend as for the heating values (see Fig. 1) can be seen. Residence time has a relatively weak influence for residence times longer than 3 h and the main influencing process parameter is temperature. In contrast to the volatile content the relative fixed carbon content is found to be influenced by both temperature and residence time increasing from 1.34 at 0.5 h to 2.13 at 12 h at 180 °C, from 2.09 at 0.5 h to 2.68 at 12 h at 230 °C and from 2.78 at 0.5 h to 2.89 at 12 h

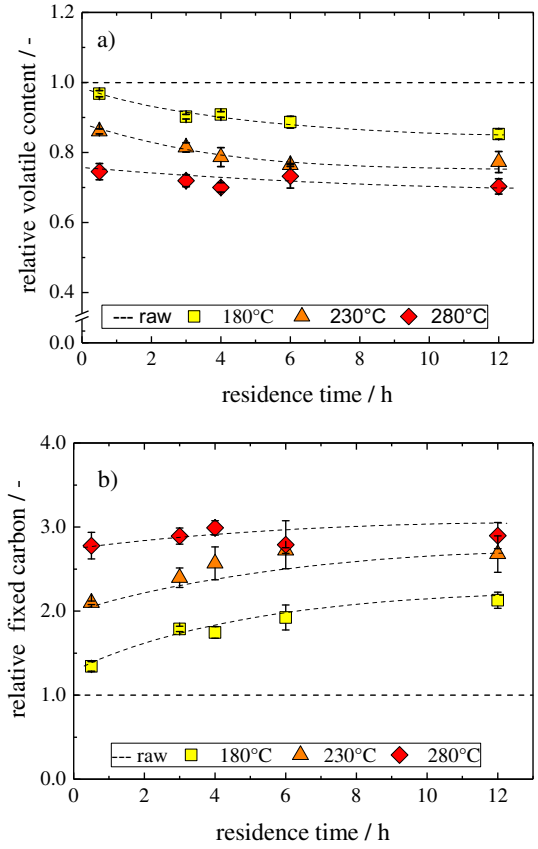

Fig. 5. Relative volatile content (figure a)) and relative fixed carbon content (figure b)) content of BSG hydrochars for reaction temperatures 180 °C, 230 °C and 280 °C versus residence time.

at 280 °C which is a significantly higher increase than the reduction of volatile content. This can be attributed to the hydrolysis of the biomass where the less stable components of the biomass which are also likely to release volatile components are dissolved whereas the more stable components form the fixed carbon.

3.2. Gasification properties

The following section discusses the reaction rate and the activation energies under CO_2 atmosphere of the hydrochars after pyrolysis. The pyrolyzed hydrochars are referred to as chars. The kinetic data for all samples is shown in Tables 2–4 for HTC reaction temperatures 180 °C, 230 °C and 280 °C.

The chars obtained from the raw BSG exhibit reaction rates of 2.78· $10^{-5}s^{-1}$ at 850 °C, 3.29· $10^{-4}s^{-1}$at 950 °C and 2.25· $10^{-3}s^{-1}$at 1050 °C at 20% conversion. These reaction rates were reduced for all chars obtained from biomass samples. In the following section the reaction rate is discussed representatively for 850 °C and 20% conversion

Table 2
Hydrochar properties and gasification reaction data for chars from raw BSG and 180 °C samples.

Residence time (h)	Raw	0.5	3	4	6	12
Fixed carbon (wt.% dry)	12.2	16.8	21.9	20.5	21.7	26.0
Volatiles (wt.% dry)	83.9	80.7	75.7	76.9	75.8	71.5
Rate 850 °C ($10^{-5}s^{-1}$)	2.78	2.70	2.20	2.11	1.85	2.13
Rate 950 °C ($10^{-4}s^{-1}$)	3.29	3.06	2.21	2.07	1.80	2.11
Rate 1050 °C ($10^{-3}s^{-1}$)	2.25	2.16	1.82	1.82	1.53	1.83
E_A (kJ kg^{-1})	271.8	271.0	272.3	275.0	272.2	274.8
$R^2_{E_A}$	0.9994	0.9998	0.9996	0.9989	0.9991	0.9991

Table 3
Hydrochar properties and gasification reaction data for chars from 230 °C samples.

Residence time (h)	0.5	3	4	6	12
Fixed carbon (wt.% dry)	25.6	29.3	29.0	33.7	32.7
Volatiles (wt.% dry)	72.2	68.4	68.3	63.8	64.8
Rate 850 °C ($10^{-5}s^{-1}$)	2.08	1.72	1.84	1.71	1.49
Rate 950 °C ($10^{-4}s^{-1}$)	3.03	1.77	1.86	1.66	1.37
Rate 1050 °C ($10^{-3}s^{-1}$)	2.24	1.21	1.25	1.04	0.84
E_A (kJ kg^{-1})	262.5	263.2	260.9	253.9	249.3
$R^2_{E_A}$	0.9987	0.9999	0.9999	0.9998	0.9999

Table 4
Hydrochar properties and gasification reaction data for chars from 280 °C samples.

Residence time (h)	0.5	3	4	6	12
Fixed carbon (wt.% dry)	34.0	35.3	37.0	32.1	35.4
Volatiles (wt.% dry)	62.5	60.4	58.0	61.4	57.8
Rate 850 °C ($10^{-5}s^{-1}$)	1.57	1.15	1.09	1.22	1.30
Rate 950 °C ($10^{-4}s^{-1}$)	1.41	0.96	0.91	1.04	1.18
Rate 1050 °C ($10^{-3}s^{-1}$)	0.74	0.64	0.56	0.68	0.86
E_A (kJ kg^{-1})	238.8	247.8	243.5	248.2	259.4
$R^2_{E_A}$	0.9990	0.9998	1.0000	0.9999	0.9997

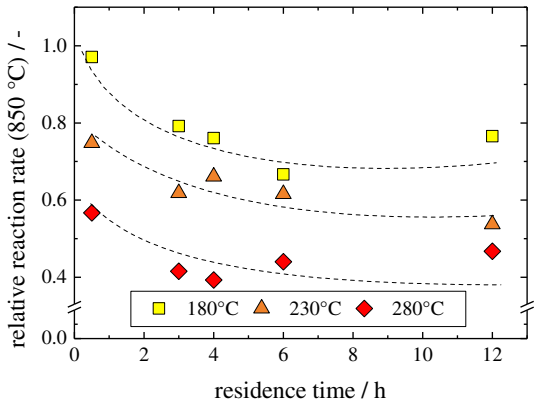

Fig. 6. Relative observed reaction rate in CO_2 atmosphere at 20% conversion of the pyrolyzed hydrochar samples versus resident time at carbonization temperatures of 180 °C, 230 °C and 280 °C at 850 °C compared to the pyrolyzed raw biomass under the same conditions.

since the same trends are found for all examined gasification temperatures. Also, for better comparison, the reaction rate is shown as a relative reaction rate according to Eq. (3). Fig. 6 shows the relative reaction rate measured at 850 °C for each char sample.

Compared to the char sample of raw biomass a reduction of the char reactivity can be observed for all carbonized samples, becoming more apparent with increasing HTC reaction severity. Similar to the fixed carbon content, the observed reaction rates are affected strongly by residence time. For carbonization temperatures of 180 °C the relative reaction rate is reduced from 0.97 at 0.5 h to 0.76 at 12 h, for 230 °C from 0.75 to 0.53 and for 280 °C from 0.57 to 0.47. The same trends can be observed at 950 °C and 1050 °C. Absolute reactivity at 850 °C and 20% conversion is shown in Tables 2–4 for all samples. The stronger influence of residence time suggests a dependence of the reaction rate on the fixed carbon content and the degree of coalification (see Fig. 3 and Fig. 5b). It is therefore possible that the char is less reactive after pyrolysis due to the formation of structures resembling anthracite or even graphite within the biomass body which have been reported by literature [27], since these structures are conserved during the pyrolysis procedure. This trend is also reported by *Laurendaeu et al.* where the authors found a reduced reactivity after pyrolysis for more uniform coal structures. The reduction was attributed to a loss of active sites for the

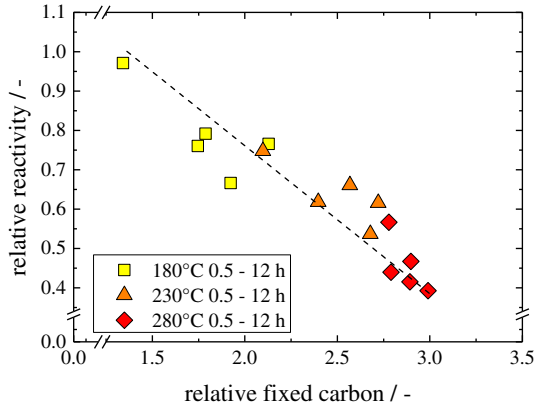

Fig. 7. Relative fixed carbon content versus relative reactivities for reaction temperatures 180 °C, 230 °C and 280 °C and residence times from 0.5 h to 12 h.

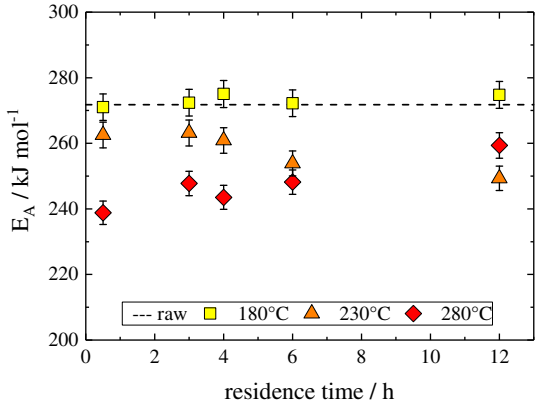

Fig. 8. Activation energy of the hydrochar samples versus resident time at carbonization temperatures of 180 °C, 230 °C and 280 °C after pyrolysis from the Arrhenius model.

CO_2 reaction due to the reduction of carbon edges, dislocations or inorganic impurities [28]. The same effect was reported by *Huo et al.* who performed pyrolysis with fuels of different coal ranks with subsequent gasification [29]. Based on this discussion, Fig. 7 shows the correlation of the relative reactivity and the relative fixed carbon content and confirms the connection between the fixed carbon content and the gasification reactivity.

The detailed correlation of these two values shows a clear linear trend and indicates, that the formation of fixed carbon directly reduces the reactivity of the chars. For the examined samples, a 2.23-fold increase of the fixed carbon content from 1.34 at 180 °C and 0.5 h to 2.99 at 280 °C and 12 h divides the relative reactivity by a similar factor of 2.41 from 0.97 to 0.39. This effect becomes more apparent for higher reaction temperatures. At 950 °C the relative reactivity is divided by a factor of 3.40 and at 1050 °C by a factor of 3.44. However, for each HTC temperature the formation of fixed carbon and hence the reduction in reactivity is significantly less pronounced for short residence times, indicated by the data points outside the groups for each HTC reaction temperature in Fig. 7. In the context of gasification this trend has to be carefully considered during selection of the pretreatment parameters, since a significant reduction of the reactivity can reduce the carbon conversion and therefore the cold gas efficiency of the gasifier. The findings in this study suggest that in combination with entrained flow gasification mild HTC conditions are favorable since the desired increased LHV and grindability can already be achieved at 180 °C with the least reduction of char reactivity.

Another indicator of carbonization effects on fuel structure are activation energies according to Arrhenius' law. The corresponding activation energies for the hydrochar samples are displayed in Fig. 8.

The chemical change of the structure of the char with carbonization reactions towards anthracite and graphite-like structures could suggest a more stable char structure and thus increased activation energies. However, the trend in Fig. 8 shows that activation energies are lowered as reaction severity increases and that the char reaction rate responds with a lower sensitivity to an increase of the gasification temperature with increasing coalification of the hydrochar sample. At 180 °C activation energy is in the range of 271– 278 kJ mol^{-1} which is in the range of the activation energy of the raw biomass with 271.8 kJ mol^{-1}. At 230 °C the activation energies are lower and decrease slightly as residence time increases from 262.5 kJ mol^{-1} to 253.9 kJ mol^{-1} at 0.5 h and 12 h respectively. The influence of residence time is reversed for 280 °C where activation energy is increased from 238.8 kJ mol^{-1} to 249.3 kJ mol^{-1} at 0.5 h and 12 h. An overview over the measured activation energies is given in Tables 2–4. The activation energies measured are comparable to semi-anthracite (209–223 kJ mol^{-1}) measured by *Roberts. et. al.* with the char prepared in a tube furnace at similar conditions [30]. Since there is currently no detailed picture of hydrochar pyrolysis with the influence of HTC-reaction conditions and the influence of the type of biomass, this topic requires further investigation. However, it has to be taken into account that the char properties are strongly influenced by pyrolysis conditions (i.e. heating rate, peak temperature) when the results regarding the char reactivity are transferred to industrial gasification applications. Studies suggest that heating rates of more than 1000 K s^{-1} during pyrolysis are not required for a realistic measurement of char reactivity [31], but this needs to be experimentally proven with uniform pyrolysis conducted in a large scale gasification setup. Also the catalytic influence of ash compounds, especially for high char conversions during gasification and their influence on the activation energy has yet to be determined.

4. Conclusions

Fuel properties of BSG hydrochars are influenced by temperature and residence time. Higher temperature and longer residence times lead to decreased mass and energy yields, higher heating values and the formation of fixed carbon in the coal. The fuel properties are more sensitive to temperature than to residence time. Main coalification mechanism is dehydration of the biomass structure. CO_2 reaction rates of chars after pyrolysis are decreased with higher reaction severity due to the formation of fixed carbon during the HTC reaction. Activation energies of the CO_2 reaction are found to decrease with higher HTC reaction severity and they are influenced stronger by temperature than residence time.

Acknowledgments

The authors would like to thank the Federal Ministry of Food and Agriculture (FKZ: 22023911) and the FNR (Fachagentur für nachwachsende Rohstoffe) for funding this work. Thank you as well to the students and workers at the institute for their support in the project.

References

[1] BMwi, Zweiter Monitoring-Bericht - Energie der Zukunft, PRpetuum GmbH, München, Berlin, 2004.
[2] T. Nieder, Zeitreihen zur Entwicklung der erneuerbaren Energien in Deutschland (1990–2014), (2015).
[3] B. Jenkins, L. Baxter, T. Miles, Combustion properties of biomass, Fuel Process. Technol. 54 (1–3) (1998) 17–46, http://dx.doi.org/10.1016/S0378-3820(97)00059-3.
[4] F. Bergius, Chemical reactions under high pressure - Nobel Lecture, Nobel Lect. Chem. (1966) 1922–1941.
[5] F. Bergius, Beitraege zur Theorie der Kohleentstehung, Naturwissenschaften 16 (1) (1928) 1–10, http://dx.doi.org/10.1007/BF01504496.
[6] A. Funke, F. Ziegler, Hydrothermal carbonization of biomass: a summary and discussion of chemical mechanisms for process engineering, Biofuels Bioprod. Biorefin. 4 (2) (2010) 160–177, http://dx.doi.org/10.1002/bbb.198.
[7] J.A. Libra, K.S. Ro, C. Kammann, A. Funke, N.D. Berge, Y. Neubauer, M.-M.

Titirici, C. Fühner, O. Bens, J. Kern, K.-H. Emmerich, Hydrothermal carbonization of biomass residuals: a comparative review of the chemistry, processes and applications of wet and dry pyrolysis, Biofuels 2 (1) (2011) 71–106, http://dx.doi.org/10.4155/bfs.10.81.

[8] C.J. Coronella, J.G. Lynam, M.T. Reza, M.H. Uddin, Hydrothermal carbonization of lignocellulosic biomass, in: F. Jin (Ed.), Green Chemistry and Sustainable Technology, Springer Berlin Heidelberg, Berlin and Heidelberg, 2014, pp. 275–311, , http://dx.doi.org/10.1007/978-3-642-54458-3_12.

[9] M.-M. Titirici, A. Funke, A. Kruse, Hydrothermal carbonization of biomass, recent advances in thermochemical conversion of biomass (2015) 325–352, http://dx.doi.org/10.1016/B978-0-444-63289-0.00012-0.

[10] Biokohle im Blick: Herstellung, Einsatz und Bewertung; [Second INTERREG NSR Biochar Conference, Berlin, 19. und 20. September 2012], in: K. Fricke (Ed.), Schriftenreihe des ANS, vol. 54, Orbit, Weimar, 2012.

[11] H.S. Kambo, A. Dutta, Strength, storage, and combustion characteristics of densified lignocellulosic biomass produced via torrefaction and hydrothermal carbonization, Appl. Energy 135 (2014) 182–191, http://dx.doi.org/10.1016/j.apenergy.2014.08.094.

[12] F. Schuchardt, K.D. Vorlop, Estimation of the carbon amount in biomass residues in Germany for hydrothermal carbonisation (HTC) and disposal of HTC-coal to the soil, Agric. For. Res. (4) (2010) 205–211.

[13] T. Herfellner, G. Bochmann, R. Meyer-Pittroff, Die Verwertung von Biertrebern - derzeitiger Stand und neue Ansätze zur energetischen Nutzung, Brauindustrie (8) (2006) 42–45.

[14] X. Lu, P.J. Pellechia, J.R. Flora, N.D. Berge, Influence of reaction time and temperature on product formation and characteristics associated with the hydrothermal carbonization of cellulose, Bioresour. Technol. 138 (2013) 180–190, http://dx.doi.org/10.1016/j.biortech.2013.03.163.

[15] S.K. Hoekman, A. Broch, C. Robbins, Hydrothermal Carbonization (HTC) of Lignocellulosic Biomass, Energy Fuel 25 (4) (2011) 1802–1810, http://dx.doi.org/10.1021/ef101745n.

[16] Z. Liu, A. Quek, S. Kent Hoekman, R. Balasubramanian, Production of solid biochar fuel from waste biomass by hydrothermal carbonization, Fuel 103 (2013) 943–949, http://dx.doi.org/10.1016/j.fuel.2012.07.069.

[17] M. Mäkelä, V. Benavente, A. Fullana, Hydrothermal carbonization of lignocellulosic biomass: effect of process conditions on hydrochar properties, Appl. Energy 155 (2015) 576–584, http://dx.doi.org/10.1016/j.apenergy.2015.06.022.

[18] S.M. Heilmann, L.R. Jader, M.J. Sadowsky, F.J. Schendel, M.G. von Keitz, K.J. Valentas, Hydrothermal carbonization of distiller's grains, Biomass Bioenergy 35 (7) (2011) 2526–2533, http://dx.doi.org/10.1016/j.biombioe.2011.02.022.

[19] I. Baskyr, B. Weiner, G. Riedel, J. Poerschmann, F.-D. Kopinke, Wet oxidation of char-water-slurries from hydrothermal carbonization of paper and brewer's spent grains, Fuel Process. Technol. 128 (2014) 425–431, http://dx.doi.org/10.1016/j.fuproc.2014.07.042.

[20] J. Poerschmann, B. Weiner, H. Wedwitschka, I. Baskyr, R. Koehler, F.-D. Kopinke, Characterization of biocoals and dissolved organic matter phases obtained upon hydrothermal carbonization of brewer's spent grain, Bioresour. Technol. 164 (2014) 162–169, http://dx.doi.org/10.1016/j.biortech.2014.04.052.

[21] A. Tremel, J. Stemann, M. Herrmann, B. Erlach, H. Spliethoff, Entrained flow gasification of biocoal from hydrothermal carbonization, Fuel 102 (2012) 396–403, http://dx.doi.org/10.1016/j.fuel.2012.05.024.

[22] D.S. Gunarathne, A. Mueller, S. Fleck, T. Kolb, J.K. Chmielewski, W. Yang, W. Blasiak, Gasification characteristics of hydrothermal carbonized biomass in an updraft pilot-scale gasifier, Energy Fuel 28 (3) (2014) 1992–2002, http://dx.doi.org/10.1021/ef402342e.

[23] H.X. Chen, N. Liu, L. Shu, R. Zong, Smoothing and differentiation of thermogravimetric data of biomass materials, J. Therm. Anal. Calorim. (78) (2004) 1029–1041.

[24] M.F. Irfan, M.R. Usman, K. Kusakabe, Coal gasification in CO2 atmosphere and its kinetics since 1948: a brief review, Energy 36 (1) (2011) 12–40, http://dx.doi.org/10.1016/j.energy.2010.10.034.

[25] K. Strauß, Kraftwerkstechnik: Zur Nutzung fossiler, nuklearer und regenerativer Energiequellen, 6th edition, VDI-Buch, Springer-Verlag Berlin Heidelberg, Berlin, Heidelberg, 2009, http://dx.doi.org/10.1007/978-3-642-01431-4.

[26] D. van Krevelen, Graphical-statistical method for the study of structure and reaction processes of coal, Fuel (29) (1950) 269–284.

[27] A. Funke, Hydrothermale Karbonisierung von Biomasse, Technische Universität Berlin, 2012.

[28] N.M. Laurendeau, Heterogeneous kinetics of coal char gasification and combustion, Prog. Energy Combust. Sci. 4 (4) (1978) 221–270, http://dx.doi.org/10.1016/0360-1285(78)90008-4.

[29] W. Huo, Z. Zhou, X. Chen, Z. Dai, G. Yu, Study on CO2 gasification reactivity and physical characteristics of biomass, petroleum coke and coal chars, Bioresour. Technol. 159 (2014) 143–149, http://dx.doi.org/10.1016/j.biortech.2014.02.117.

[30] D.G. Roberts, D.J. Harris, Char gasification with O 2, CO 2, and H 2 O: effects of pressure on intrinsic reaction kinetics, Energy Fuel 14 (2) (2000) 483–489, http://dx.doi.org/10.1021/ef9901894.

[31] C.J. Hindmarsh, K.M. Thomas, W.X. Wang, H.Y. Cai, A.J. Güell, D.R. Dugwell, R. Kandiyoti, A comparison of the pyrolysis of coal in wire-mesh and entrained-flow reactors, Fuel 74 (8) (1995) 1185–1190, http://dx.doi.org/10.1016/0016-2361(95)00036-5.